# SARS-CoV-2: A Study of the Dispersion Characteristics of Aerosol Particles Using Ultrafast Carbon Nanotube Sensors in a Simulated Indoor Environment (A Novel Technique)

**Shriya Kapoor**

*Spring Valley High School, Columbia, SC*

The SARS-CoV-2 virus (COVID-19) pandemic has exposed the lack of preparedness of many advanced countries and their methodology to bring it under control. Understanding the trajectory and spread pattern of virus carrying airborne respiratory aerosol droplets with quantifiable data can solidify or negate the guidelines for social distancing, and disease control and spread. Carbon nanotubes (CNT) sensors, CSM-eSTEP cough stimulator, optical particle sizer, and a particle image velocimetry (PIV) were used to: a) quantify velocity of exhaled air from cough under normal physiological condition, b) evaluate and quantify transport of aerosol particles from a simulated cough and c) dispersion characteristics of aerosol droplets within the six feet to validate guidelines set by CDC. This experimental trial validated that a cough (teenager and adult) air flow pressure is equivalent to 30-50 PSI compressed air flow from an orifice. The cough air flow trajectory was found to be detectable and quantifiable by sensors as far as 1.3 meters away from source. Further experimentation revealed a statistically high number (10 cm away, $F(2,87)=4.76$, $p<0.012$, and 1.8 m away, $F(2,87) = 4.18$, $p<0.018$) of aerosols particles detected beyond the social distance guideline set by CDC. Lastly, the PIV and velocity vectors reveal the disorderly spread of the aerosol particles thus requiring thorough sanitization in addition to social distancing guidelines. In the future, different indoor criteria of humidity, temperature and HVAC air flow will be set to understand virus laden aerosol velocity vectors.

## Introduction

Fear continues to intensify on the account of the constant surge in cases of the novel airborne virus, SARS-CoV-2 virus, or widely known as the coronavirus (COVID-19). Originating from Wuhan, China, the SARS-CoV-2 virus rapidly crossed Chinese borders, escalating to a global pandemic and ultimately residing in the United States, renouncing it as the center of the pandemic. The SARS-CoV-2 virus has infected over 181 million cases globally with 3.93 million deaths as of June 2021 and is continuing to increase at an alarming rate by the day despite numerous guidelines that are put in place to curb the spread. The question here is: why is this disease not coming under control? Researchers are continuing to understand the trajectory of the virus to assist in disease control and spread (COVID-19 Map); that is why it is crucial to understand the vectors in the release of pulmonary pathogen laden muco-salivary fluids through a medium in terms of short-range and long-range aerosol droplet travel. Understanding this process will help with safety measures and guidelines on social behavior, personal hygiene, wearing masks, pre, and post-use sanitization, social distancing, and limitations on indoor and outdoor gatherings/activities.

The Centers for Disease Control and Prevention (CDC), a public health institute, has inadequately equipped the public with information regarding the spread of the SARS-CoV-2 virus through particle characteristics. The CDC provides businesses, schools, offices, and places of public gathering, etc, compliance information stating mere inferences regarding the spread of the SARS-CoV-2 virus; such as, only stating an approximation that indoor ventilation systems and HVAC systems are more likely susceptible to disease spread and progression (personal and social activities). In addition, guidelines enforced by the CDC provide details and the nomenclature of disease progression only through fomite or contact surfaces, rather than close and long-range airborne virus proximities through several years of research and guidance in virology and germ theory. In fact, the CDC states, "there is growing evidence that droplets and airborne particles can remain suspended in the air and be inhaled by others in close proximity and can travel distances beyond six feet (for example, during choir practice, loud talking in restaurants, or heavy breathing in fitness classes)" (Jon, 2020). Emphasis is relied on the term, "growing evidence," bringing to attention the unknown information about the airborne spread of the SARS-CoV-2 virus in long-range distances, contaminated surfaces, and points of accumulation in indoor conditions. This creates rising interest in understanding: 1) the mechanics of exhalation that induces the highest velocity to aerosol droplets carrying the virus, i.e, screaming, coughing, or sneezing, 2) indoor occupancy density (area per person) in places like offices, school classroom, department stores, etc. vs places where activities lead to physiological stress such as fitness center, indoor stadiums, or places of worship, 3) how the air travels through various indoor environments, its flow characteristics; such as, size and amount of aerosol suspension in the air that affect the transmission of virus/ aerosol particles and 4) decontamination process of commonplaces of use such as toilets, door handles/knobs, tables and chairs and indoor air vents.

Many researchers have relied on previously completed research parameters with varying test criteria to develop their understanding of aerosol particle travel or by computer-simulated flow analysis. Specifically, the researchers create test models to understand how far the aerosol particles can potentially travel through piecing together parameters from several previously completed research. Not enough information is available from the researched articles that link the critical characteristics such as air flow pressure from cough, aerosol particle ejection velocity vectors, and spread patterns through the use of fast response sensors.

Therefore, the purpose of this research is to quantitatively define characteristics of how airborne virus particles travel short-range and long-range distances after an initial cough by a virus-host, essentially testing particle viability and profile. This research utilizes ultrafast carbon nanotube (CNT) flex and humidity sensors to first, measure actual breath exhalation and coughing pressure of two subjects to experimentally calibrate and simulate a human cough using a CSM-eSTEP and blaustein atomizing module (BLAM). This setup was intended to provide fast reliable data to map aerosol movement in time scale. Secondly, an optical particle sizer was used to measure aerosol particle size and dispersion rate over a distance of 1.8 m (6 feet - CDC guideline); and lastly, a particle image velocimetry (PIV) to validate the flow and velocity vector patterns for maximum accuracy and precision of recorded test data. Carbon nanotubes and the PIV system helped analyze and calculate the flow rate of aerosol and characteristics of particle profiles. This consists of calculating particle velocity, size, distribution, dispersion trends, and pressure peaks in particle dispersion in relation to time. If successful with this project, both qualitative and quantitative characteristics of exhalation from coughing along with characterizing particle parameter can assist in solidifying the ever-changing regulations for social distancing, wearing masks, and opening schools, offices, businesses, restaurants, and etc. to help decrease the disorderly spread of the SARS-CoV-2 virus.

**Experimental Goal:**

1. When the CNT flex sensors were placed 10 cm from two participants under normal physiological conditions, the sensor's signal pattern could accurately measure a cough's pressure characteristics. This signal was matched to pressure release from compressed air to simulate an experimental cough using CSM-eStep and BLAM.
2. When the placement of CNT flex sensors were gradually increased in axial distance away from a CSMe-STEP (cough simulator), then the sensor's signal pattern was able to measure a cough's pressure and aerosol decay over an increasing distance and accurately assess the detectable distance traveled by aerosol under the velocity of air flow.
3. If two optical particle sizers were placed 10 cm and 1.8 m (6ft) apart from a BLAM orifice, then the quantity of aerosol particles and their sizes relative to the ambient room humidity particle number were measured to validate CDC guidelines.
4. When a PIV (particle image velocimetry) was used to capture the aerosol particles released from the CSMe-STEP, then the MATLAB's PIVlab software assisted in determining particle velocity vectors and particle trajectories.

Airborne diseases consist of either an airborne virus (agent that hosts on human cells), bacteria (a microorganism), or fungi (spore-producing organism). Most commonly, airborne pulmonary diseases spread when someone speaks, coughs, sneezes, or spews their nasal or throat cavity mucus, making disease control challenging. Intense exhalation processes such as coughing and sneezing results in multiphase spewing clouds of moist air suspended droplets as vectors in the fastest transmission of pathogens. When a virus, bacteria laden particle, is coughed, the pathogen attaches to moisture particles through the air until it is introduced to another recipient to host on (Osborn, 2020). Worldwide guidelines currently state that when someone coughs or sneezes, it can spread up to 6 feet (1.8 m) (Stinchcombe). In addition, CDC has enforced all social distancing guidelines to a 6 feet (1.8 meter) distance between people in common areas.

Qian et al. from the Southeast University School of Energy and Environment completed a study that was published in the Journal of Thoracic Disease and concluded the rudimentary knowledge of how virus droplets travel through the air. It was stated that when one sneezes or coughs, large amounts of moist particles, also known as large mucosa droplets, are released from the mouth or nose. These droplets tend to fall downward as influenced by gravitational forces, have a large diameter (for particles to be characterized as a large droplet, they must have a diameter of >5μm (microns)), and greater volume. However, some droplets will then dry out and attach to small particles of moisture through the air, in which they become droplet nuclei and can survive and remain in the air for long periods of time (Qian et al., 2018). Droplet nuclei because of their smaller volume and size, are predicted to travel farther because they have a smaller diameter and can be easily influenced by their surrounding environment (air, wind, vents). It is stated that droplet nuclei normally have a size of <0.5μm. When a particle reaches a diameter of <5μm it is characterized as an aerosol, therefore, droplet nuclei are a category of aerosols. However, measurable data has not been provided in understanding particle characteristics of droplet nuclei. For example, a study completed at the Massachusetts Institute of Technology (MIT) suggests that pathogen ridded aerosols can travel farther than most scientists expected (Bourouiba et al., 2013). This study at MIT, mathematically models how far aerosols travel, by using various patterns noticed from parameters found in other research. Specifically, this research fails to consider distinct and detailed time frameworks as aerosols diffuse from a cough, accumulation of exact particle size, velocity vectors, and an estimate of the number of particles from a vertical and horizontal projection through data collection. In addition, a study completed at the University of Nicosia stated that coughs without the influence of wind supposedly travel less than 1 meter (m) in distance because all the large droplets and droplet nucleus fall to the ground within 0.12 - 0.2 seconds by the influence of gravity (Dbouk et al., 2005). The paper further shows that only increased wind between 4-12 kilometers per hour (km/h) allows particles to travel up to 6 m. This research, instead, focuses on validating the research findings under still environmental conditions. In addition, the researchers, state that they were unable to quantify the size of droplets that were released from their developed orifice, to further analyze the particle vectors.

When a cough is released from a person's mouth (simulated as pressurized moisture released through an orifice), it has an initial momentum. This can also be referred to as an initial thrust, allowing for buoyant droplets of aerosols to project upward against its weight and the force of gravity. This initial buoyancy creates a cough cloud, as shown in Figure 1. The initial density and pressure in the cough cloud is higher because there is an increase in crowdedness and as time progresses the pressure and velocity continue to decrease rapidly. According to Wei et al., the cough jet is characterized by two stages: the starting jet termed as direct spray region that occurs between 1-2 m from the source and the turbulent jet is dissolved in the room airflow that exists beyond 2 m (Wei et al., 2016). It is this second region of contamination that is of significance and much less is understood in terms of spread mechanism and control of the exposure. The first region data has to be validated to support the possibility of having a higher quantity of aerosol in the second region.

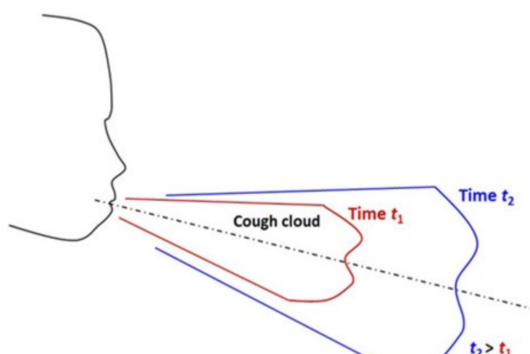


Figure 1 shows projection of a cough cloud traveling linearly

Mechanics of cough, as explained in, "The Gross Science of a Cough and a Sneeze", has various characteristics such as short, long, deep, and stifled, and carries varied amounts of body fluid as moisture or aerosol. Cough is a process of the body's reflux to rid irritants and prevent infections. The process first starts with a deep breath, an accumulation of expiratory volume is generated from a compression of air in the lungs and finally a forced release of air and saliva aerosol droplets through the mouth/orifice. Human saliva is a complex homogeneous fluid mixture of many volatile organic compounds such as salts, proteins and fatty acids in 97% water (Turner et al., 2006). This indicates that most of the content released when coughed, is composed of water, ridden with pathogens, and macromolecules. One cough produces approximately 0.6 to 1.6 L (liters) of airflow with an exit velocity of 10 m/s in a duration of 0.5 second. It can be assumed that the cough flow is analogous to laminar flow in the first stage of ejection and then becomes an interrupted jet. Other researchers have measured that the flow rate of droplets and aerosols, or the rate at which a cough is released, is approximately 0.1 mL/minute. Common parameters for pressure release for a cough, vary significantly according to previously completed research (Yuguo, 2017).

In addition, these aerosols and large particles are initially carried through pressure released in relation to a patient's muscle contraction of the chest and abdomen. The pressure initially released from the orifice will decay as the particles travel further and further, gradually decreasing the velocity of the particles and as time progresses from the initial cough. The modeling of this cough process is similar to that of velocity of pressurized air escaping from an orifice and can be defined as: (velocity escaping compressed air)

$$v_2 = \sqrt{2g \cdot \frac{k}{k-1} \cdot 53.3(459.7 + F)\left[1 - \left(\frac{p_2}{p_1}\right)^{\frac{k-1}{k}}\right]}$$

Where V2 is the velocity escaping air in m/sec, g is acceleration due to gravity (9.8 m/s^2, 32.16 ft/sec^2), k is 1.41 or the coefficient of compressed air, F is the temperature in degrees F, p2 is the atmospheric pressure (1 bar or 14.7 pounds per square inch (PSI)), and p1 is the pressure of air released from the compressed air container in bar/PSI (Engineers Edge, 2017).

In this research, carbon nanotube sensors (CNT) were used to receive fast response data as well as understanding the time delay when particles reach certain distances after an initial simulated cough. Carbon nanotubes are adaptile rolled up sheets of hexagonal crystal lattices or graphene. They can be either categorized as a single-walled or a multi-walled carbon nanotubes. Single-walled carbon nanotubes have unique chirality and multi-walled carbon nanotubes have a high aspect ratio allowing them to have properties such as fast response time, mechanical strength, high carrying capacities, transparency, and high thermal conductivity (Wei et al., 2017). Specifically, multi-walled carbon nanotubes have a high aspect ratio or fast response time due to the increase in holes throughout the sheets of hexagonal crystal lattices allowing to absorb maximum material and signals from external forces (Ossola, 2015). This technology has recently been used in sensors due to their stiffness, robustness, elasticity, sensitivity, and fast response time (Electrical4U, 2020). These sensors have a response time of under 30 milliseconds, proven to be one of the fastest sensors available, allowing the CNT flex and humidity sensor to be able to accurately detect the time it takes for the particles to travel a set distance in milliseconds. In comparison, as shown in Figure 2, commonly sold sensors by Sensirion Sensors (a popular sensor company) have their fastest sensor, a Mass Flow Meter SPM3000, at a response rate of only 0.5 seconds (Digital Humidity Sensor SHT85 (RH/T)), hindering the accuracy of the sensors.


Figure 2 displays different types of Sensirion Sensors and their corresponding response rates. ("Digital Humidity Sensor SHT85 (RH/T)")

Due to the fast response time of CNT humidity and flex sensor, they can be integrated for the purpose of understanding real time variation in pressure and humidity as a correlation for particle flow pressure and accumulation. In addition, the carbon nanotubes will also be placed in a linear flow path to understand the time the aerosol particles take to travel and what potential they have of reaching certain areas and extents to determine length of distance traveled to assist in creating a particle profile.

A CSM-eSTEP (a puff generation machine) at the University of South Carolina lab was utilized to mechanically generate cough-like conditions at a predetermined adjustable pressure and flow rate for aerosol generation. The CSM-eSTEP is a driven control box with timer controller and valve operated by positive pressure (canister pressure is maintained within the system and is released in immediate surroundings when a valve opens). The CSM-eSTEP is connected to an compressed air cylinder, an automated syringe pump for metered liquid (water) delivery and a blaustein atomizing module (BLAM) orifice to imitate a human cough. This system mimics a human cough and for fixed flow rates and pressure.

An optical particle sizer was utilized to understand the size of particles and the number of particles that can travel certain set distances. The optical particle sizer is a spectrometer that can categorize aerosol particle sizes at a 120-degree light into various size bins. Specifically, the optical particle sizer can sort particles and aerosols between the sizes of 0.3 to 10 µm through 16 channels and 10 bins (Optical Particle Sizer 3330). Due to the accuracy and specificity of the optical particle sizer, the distance of a cough can be measured, and the viability of pressure decay, diffusion, and horizontal and vertical trajectory can be supported.

For this research project, a particle image velocimetry (PIV) at the University of South Carolina Lab will be used, similar to the research by Nishimura et al., 2013. A PIV is a method that allows for close 2D visualization of a space frame through a high-speed camera and a laser beam allowing for accurate understanding of particle location. The PIV will allow for a visual understanding of the particle flow characteristics through multiple picture frames of the aerosol particles by taking photographs at a time difference to calculate the average/common velocity field. The laser beam in the PIV focuses on the targeted area for a picture by creating a light sheet and illuminating the aerosol particle, perpendicular to the PIV, allowing the camera(s) to take the image. These pictures taken will then be analyzed through the PIV computer program, LAVISION-8 (Sick et al., 2013) and MATLAB program, PIVLab.

## Methods

### Initial Parameter and Experimental Setup:

To conduct this research, a LabVIEW program, as shown in Figure 3, was developed and programmed to connect CNT sensors and for data collection and graphical visualization. The LabVIEW program consists of the multiple tabs for easy menu navigation. The first tab: the Sensor Setting screen for selecting the sensors and attaching to the four channels of choice to the Teensy controller that allows for sensor calibration. The second tab: the DAQ tab to graphically monitor the signal on all four channels. The third tab: a data processing tab for data analysis and also allowed to have additional peripheral equipment to be controlled for equipment synchronization.

**Figure 3: LabVIEW Block Diagram and Front Panel DAQ**

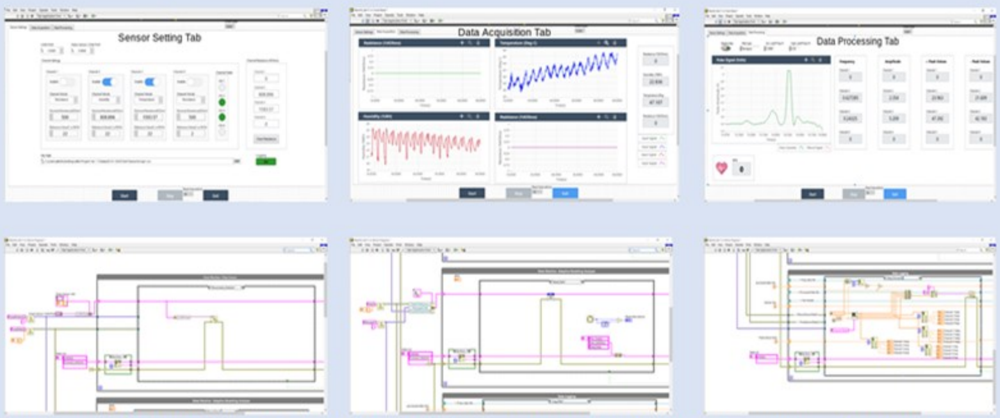


Figure 3 shows the 3 back panel photos of the LabVIEW DAQ program code and the other three show the front panel sensor setting tab, data acquisition tab, and data processing tab.

### Part 1. Setup of Simulated Cough Conditions:

The first part of this study was to measure actual cough air pressure and amount of moisture released using a CNT flex and humidity sensors. The significance of this experiment was to understand the characteristics of exhalation and coughing and how this process can be simulated in a lab setting for accurately determining aerosol borne viral spread. This trial was performed only on two subjects (due to COVID restrictions), an adult (AK) and a teenager (SK) to understand the difference in pressure and moisture released from an actual cough. Pressure was measured as deflection of the flex sensor and humidity as percent change from ambient. Each subject had to cough 6 to 8 times in front of the sensors that were kept approximately 10 centimeters away from the mouth for three sets of data from each subject. Data was collected and tabulated using Microsoft Excel. Each data logging set was marked, "SK and AK Cough Set 1,2, or 3," and repeated until three sets of data collection were completed.

The second step was to use this actual cough pressure data and humidity value from the researched article, and create a laboratory setting to simulate human cough using a controlled pressure release from a compressed air cylinder, CSM-eStep, and BLAM atomizer. Pressure setting from the air cylinder was changed from a starting pressure of 1.0344 bar (15PSI) and an incremental step of 0.344 bar (5PSI) to final pressure of 3.8 bar (50PSI). ***Here on all the pressure units will be PSI for simplicity, but for calculations values were converted to SI***. The CSM-eSTEP was then set at 5 second between each cough for periods of 60 seconds. A calibrated flex sensor was placed 10 cm away from the orifice. The LabVIEW program was started, and data logging was turned on where data was collected for 60 seconds while the CSM-eSTEP simulator was running. The cough air pressure of the teen and adult cough was then matched with the pressure step from the simulated trials. The experimental set up was completed to establish the baseline of cough for easy cough stimulation. All trials were repeated five times for data accuracy.

### Part 2. Simulating Cough Air Pressure and Aerosol Decay Study

The second part of this experiment was to understand the pressure and moisture decay over an increasing point of impact distance of 10 to 110 cm. The significance of this experiment was to scientifically provide evidence of how far the pressurized airflow exiting the source exhibits laminar flow before getting diffused, thus understanding the aerosol spread in each space due to coughing. For consistent data collection, a sensor mounting fixture was created, as shown in Figure 4, to hold two flex sensors, that were placed in front of the CSM-eSTEP. Next, the CSM-eSTEP (sneeze/ cough stimulator) was set up and calibrated with the use of the pressure gauge and bottle tank, metal syringe, mechanical syringe pusher, and atomizer as shown in Figure 5.

The air pressure was set at 30 PSI for the first trial and 40PSI for the second trial on the CSM-estep with a 5 second interval cough gap for a 60 seconds trial period. The CSM-eSTEP program was started and data logging was turned on where data was collected for 60 seconds. These trials were repeated by moving the mount 10 cm away from the BLAM nozzle and data recorded for 60 trials. A total of 8 trials were conducted and data logged until a distance of 80 cm and 110 cm was reached away from the BLAM orifice. When the two sensors were placed at a fixed distance of 30 cm apart, the time delayed sensor signal response from the first closest sensor (10 cm) to the second sensor signal was used to calculate the cough air flow speed travel of 30 cm and the data was analyzed for all 8 trials by averaging the results.

### Part 3. Optical Particle Sizer for aerosol particle count:

In this part of the experiment, the sensor mounted fixture, CSM-eSTEP, mechanical syringe pusher, BLAM, metal syringe, and LabVIEW program (Figure 5) were utilized with an optical particle counter (Figure 6). The goal of this experiment is to use the results from part 1 and 2 to quantify the aerosol particle count to validate or recommend the social distance guidelines established by CDC.

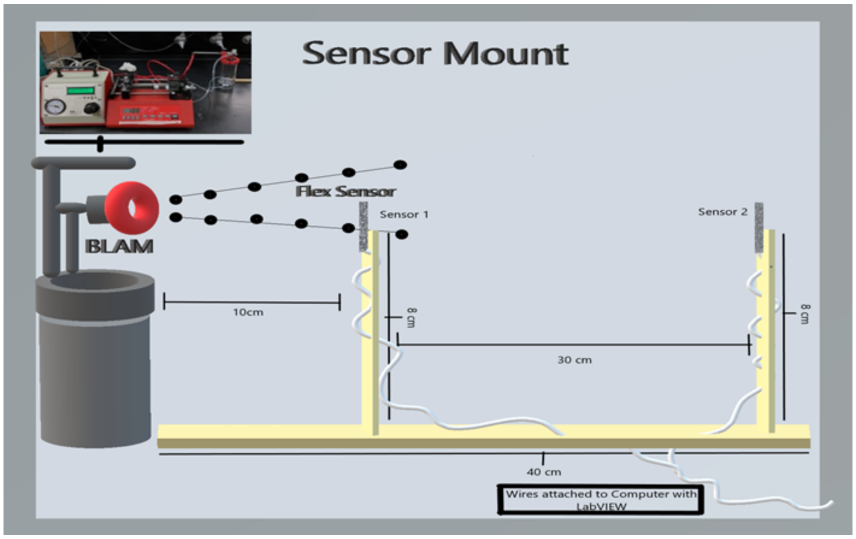


Figure 4 is the wooden mount created and the attached flex sensors.

Figure 5: CSM-eSTEP, Syringe, Mechanical Syringe Pusher, and BLAM

Figure 5 shows the connection between the mechanical syringe pusher and the CSM-eSTEP which is powered by a pressure tank

Figure 6: Optical Particle Counter Scheduling

Figure 6 shows the Optical particle counter settings and pre-test parameters

Additionally, along with the flex sensors, an additional carbon nanotube humidity sensor was placed in channel 2 of the connecting teensy aurdino wires, 10 cm away from the BLAM. The same parameters of 30 PSI and 40 PSI pressure were released and a 0.1mm/min flow rate were repeated and set on the CSM-eSTEP and mechanical syringe pusher. The first optical particle sizer tube was attached next to the flex and humidity sensor, therefore, the humidity sensor, flex sensor, and optical particle sizer were all 10 cm away from the BLAM. The other optical particle sizer was placed 1.8 m away (6 feet to mark CDC guidelines) linearly. On the optical particle sizers, the data collection rate was at 1 second for a total of 90 seconds shown above in Figure 6. The sensors were calibrated, and data logging was turned on the LabVIEW software along with all the other equipment at the same time and data was collected for a total of 3 times.

This data was then tabulated in Microsoft Excel. The particles count data under each aerosol size bin was tabulated from 16 channels and 10 bins from 10 cm to 1.8 m (6 ft) into a one-way ANOVA for each of the 3 trials. Additionally, a post hoc Tukey test was performed and interaction plots were created.

**Part 4. Particle Image Velocimetry (PIV):**

Lastly, a PIV was used along with the CSMe-STEP, mechanical syringe pusher, BLAM, and a green beam laser to take high speed photos of the particle and aerosol trajectories as shown in Figure 7. The main purpose of this last experiment is to use simulated aerosol dispersion along with PIV to establish aerosol travel trajectory. For this part of the experimentation at the University of South Carolina, a large clear test chamber was used. The two PIV cameras were positioned perpendicular to the green beam light laser and directly opposite to BLAM. The distance between two cameras was set 30 cm apart and calibrated to a 30 cm straight line inside of the ventilation chamber. The computer system connected to LaVISION 8 software, PIV cameras were set at 50000us double frame mode, with a trigger rate and image rate of 5.33 Hz, and a recording length of 31 images for a duration of 5.821 seconds (each cough from the CSMe-STEP and BLAM was for 5 second periods). For safety, the caution laser light was turned on outside of the lab and everyone present in the lab room was required to wear safety glasses. The laser light was then turned on as shown in Figure 8. The CSMe-STEP was started 5 times and after every 30 second interval, the PIV captured 31 images per trial. The picture frames were uploaded in MATLAB's PIVlab processor to analyze frame sequences and calculate velocity vectors.

Figure 7: PIV data collection equipment setup

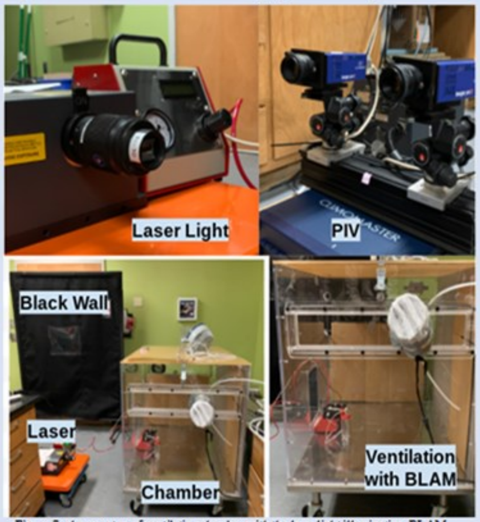


Figure 7: shows setup of ventilation chamber with the laser light illumination, BLAM, and PIV cameras.

Figure 8: Laser illumination and starting of PIV data collection

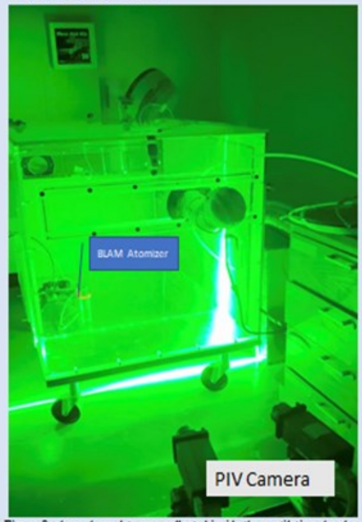


Figure 8: shows how data was collected inside the ventilation chamber with the laser light illumination, BLAM, and PIV cameras.

## Results

### Part 1. Simulated Cough Conditions Results:

As stated in part 1 of this experiment, the goal was to determine the pressure required from the CSM-eSTEP that would best represent a cough signal. The best match data was selected, and the graphs were overlaid for comparison of flex sensor's resistance of human cough and orifice pressure trials. As shown in the Figure 9, data was overlaid comparing SK cough to a 30 PSI pressure from the BLAM. The cough expended from participant SK is depicted on the primary axis with the blue line while the 30 PSI pressure is depicted by the orange line on the secondary axis. The SK cough averaged at 0.4 Ω (ohms) higher than the 30 PSI. Figure 9 accurately compares the pressure release from participant SK (blue line on primary axis), and the sensor deflection/bend resistance at 40 PSI released from the BLAM (orange line on secondary axis) was higher. The primary axis, SK cough, ranges between 220 to 223 Ω. On the secondary axis, the resistance in Ω, ranges between 227 to 230 Ω. The average change in resistance(Ω) between SK participant and 40 PSI pressure was approximately 0.9 Ω. This presents a large difference between flex on the sensor from the cough of SK participant and by a 40 PSI pressure.

Figure 9: SK Cough compared to 30 PSI


Figure 9 shows the correlation between SK cough and 40 PSI. The resistance was calculated through the use of a flex sensor placed 10 cm away from the 40 PSI pressure and SK participant.

However, since ranges of coughs can vary significantly based on a participants age, lung volume, and cough characteristic, a second subject, an adult, AK's cough signal, was recorded and the same trials were repeated using compressed air and CSM-eSTEP with increasing pressures. Figure 10 shows the comparison of the pressure release from participant AK, blue line on primary axis, and the flex resistance at 40 PSI released from the BLAM, orange line on secondary axis. The primary axis, AK cough, ranges between 219 to 223 Ω (ohms). The secondary axis, resistance in Ω, ranges between 226.6 to 230.6 Ω. The average change in Ω between AK participant and 40 PSI pressure was approximately 1.2 Ω. In contrast to SK cough and 40 PSI, AK cough expended more resistance than 40 PSI.

The results clearly show that for cough air pressure, signal data measured as flex sensor deflection is a reliable method to analyze cough cycle. Depending on the cough of a teenager and an adult, the air pressure release test from the compressed air tank closely matches between the low pressure of 30 PSI and high pressure of 40 PSI respectively. Some AK cough pressure signals were higher than the 40 PSI value while SK cough pressure signals were between 30- 40 PSI, it was estimated that a PSI level of 30-40 PSI would be most appropriate to represent a human cough.

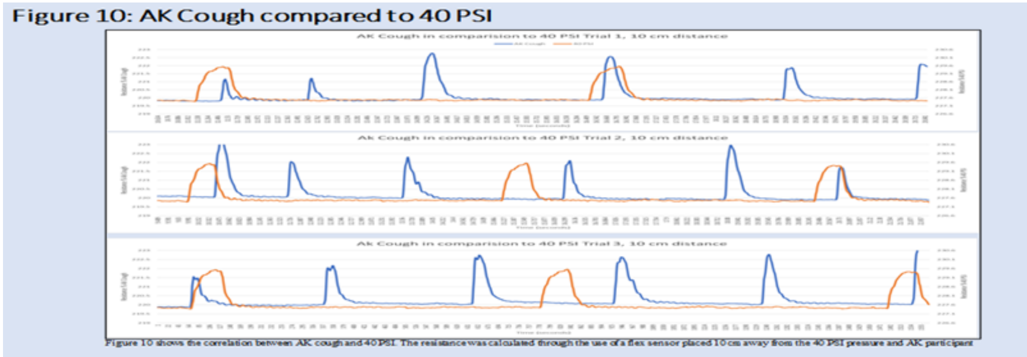

Figure 10 shows the correlation between AK cough and 40 PSI. The resistance was calculated through the use of a flex sensor placed 10 cm away from the 40 PSI pressure and AK participant

**Part 2. Simulated Cough Air Pressure and Aerosol Decay Study**

The time delay of bend signal from two flex sensors placed 30 cm apart on an axial plane from the BLAM nozzle, was used to calculate the pressure diffusion over time, and the sensors were subject to a releasing pressure of 30 PSI and 40 PSI (approximated as a simulated cough). Figure 11 shows the signal plot from the trials with increasing distance of sensor away from BLAM nozzle until a final distance of 80 cm and 110 cm is achieved. Analysis of these graphical data also shows two critical experimental information a) intensity of the signal (nominal value to peak value) and b) amplitude of the signal (width of the signal wave). As it can be seen that with fixed air pressure of 30 and 40 PSI, the signal intensity continues to drop as the distance of the sensors increases from the BLAM orifice. The time difference, shown in Figure 12, was calculated between each visible peak between each 30 cm distance. Calculating the pressure peaks over time allows for the comparative analysis of how long it takes for the pressure simulating a cough to travel certain distances. This data also allows for the interpretation of the time decay as the distance increases. Max peaks for graph distance of 70-100 cm and 80-110 cm were incoherent due to weak signal, therefore, were excluded from data analysis and time peak to peak averages. When the flex sensors were placed 20 cm and 50 cm apart, the time difference between start of first signal to the start of second signal was 0.125 seconds. Similar calculations were done with increasing distances 30-60 cm, 40-70 cm, 50-80 cm, where the time difference was 0.2066 seconds, 0.2262 seconds, 0.2141 seconds, and 0.2478 seconds respectively. This shows that as the distance increased, the pressure intensity decreased and hence the time gap increased. This data analysis was repeated for 40 PSI which as shown in Figure 13.

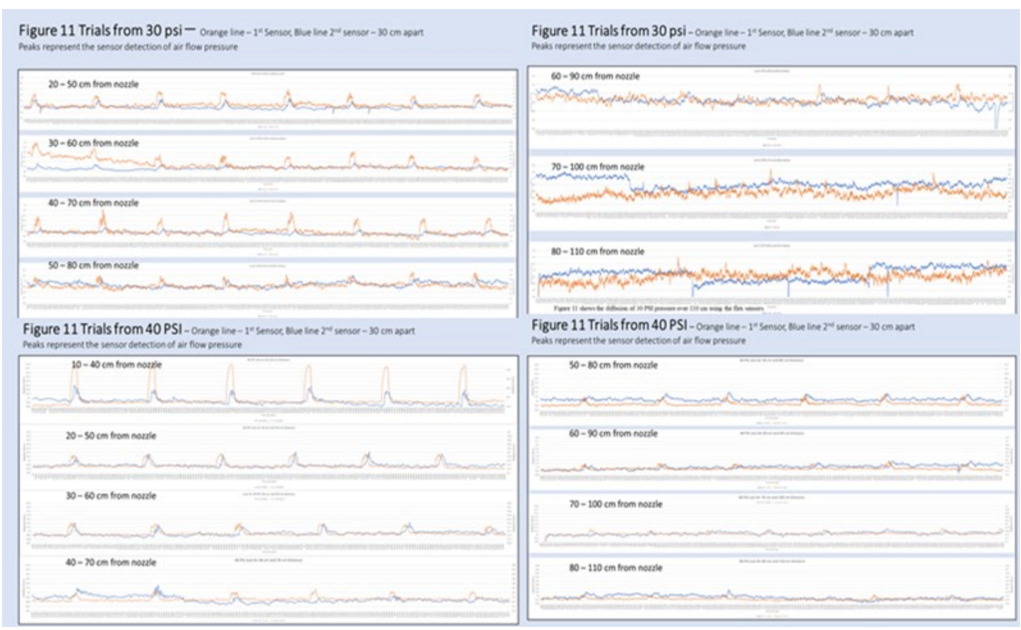


When the flex sensors were placed 10 cm and 40 cm apart, the time difference between start of first signal to the start of second signal was 0.1048 seconds. Similar calculations were done with increasing distances 20-50 cm, 30-60 cm, 40-70 cm, 50-80 cm, the time difference was 0.1858 seconds, 0.2063 seconds, 0.2252 seconds, 0.2738 seconds, respectively. Data from 40 PSI also shows that as the distance increased, the pressure intensity decreased, and the flow was clearly detectable as far away up to 110 cm. In conclusion, for both 30 PSI and 40 PSI, as the distance increased, the pressure decreased, but still detectable to conclude that there is enough kinetic energy to carry aerosol particles. The peak value of the pressure was calculated to understand the initial kinetic velocity induced in air due to pressure and decay over 30 cm. Using the velocity escaping compressed air equation, the velocity of air escaping from the orifice at 30PSI was 310 m/s and quickly decreased to 15.3 m/s after a distance of 30 cm and at 40PSI the velocity was 325 m/s decreasing to 14 m/s after a distance of 30 cm .

**Part 3. Aerosol particle count using Optical Particle Sizer:**

Figure 14, shows the aerosol travel distance as detected by flex, humidity and OPS system combined. To understand aerosol particle size and horizontal distribution, a one-way ANOVA was performed on data collected by the optical particle sizers, one from 30 cm (1 ft) away from the BLAM and the other 1.8 m (6ft) away from the BLAM. There were a total of 3 trials, each trial was recorded in both optical particle sizers. The distribution of the particles were graphed on Microsoft Excel as shown bottom part of Figure 15.

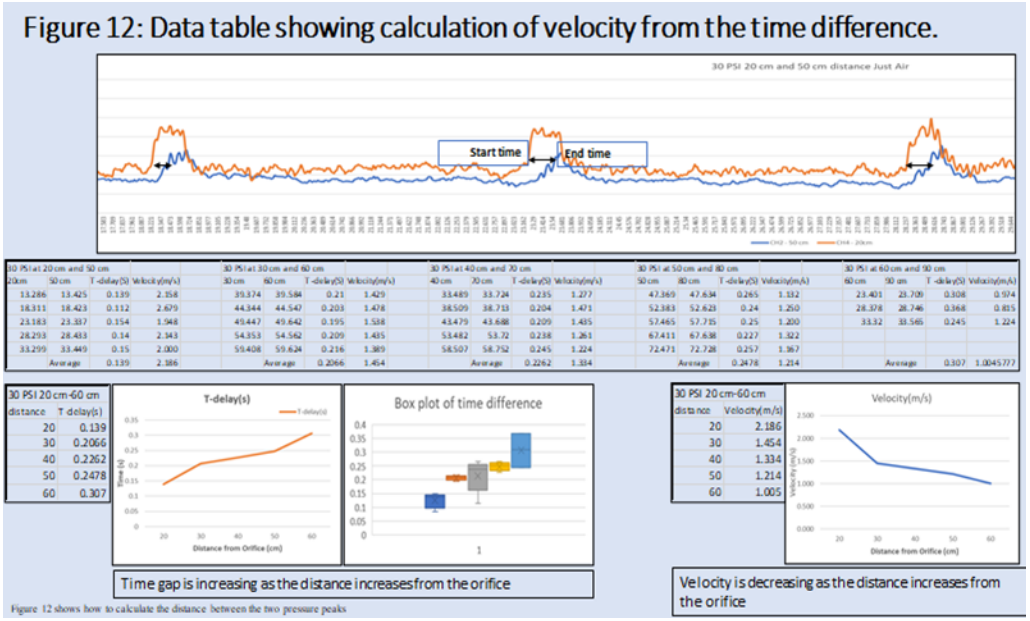

Figure 12: Data table showing calculation of velocity from the time difference.

Figure 12 shows how to calculate the distance between the two pressure peaks

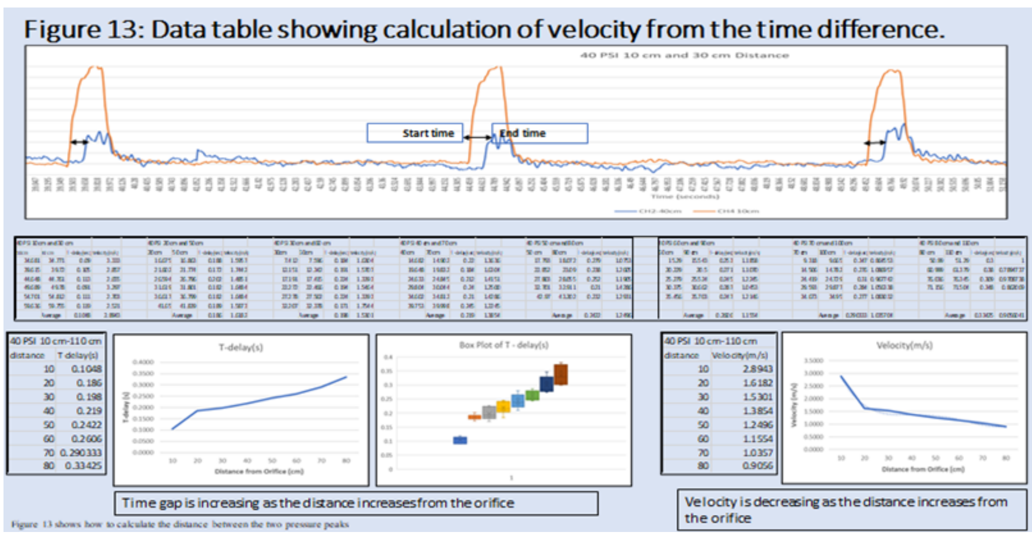

Figure 13: Data table showing calculation of velocity from the time difference.

Figure 13 shows how to calculate the distance between the two pressure peaks

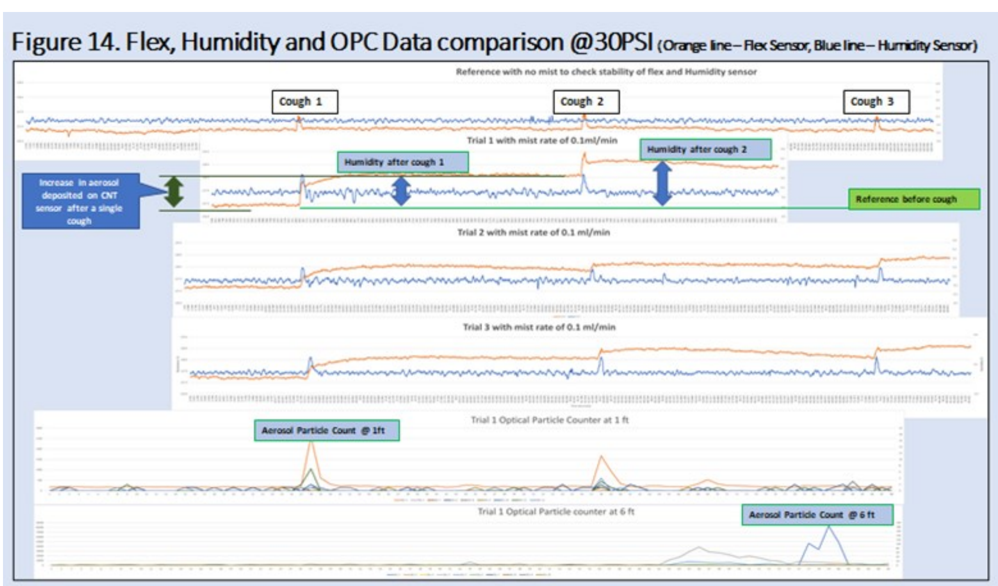

Figure 14. Flex, Humidity and OPC Data comparison @30PSI (Orange line – Flex Sensor, Blue line – Humidity Sensor)

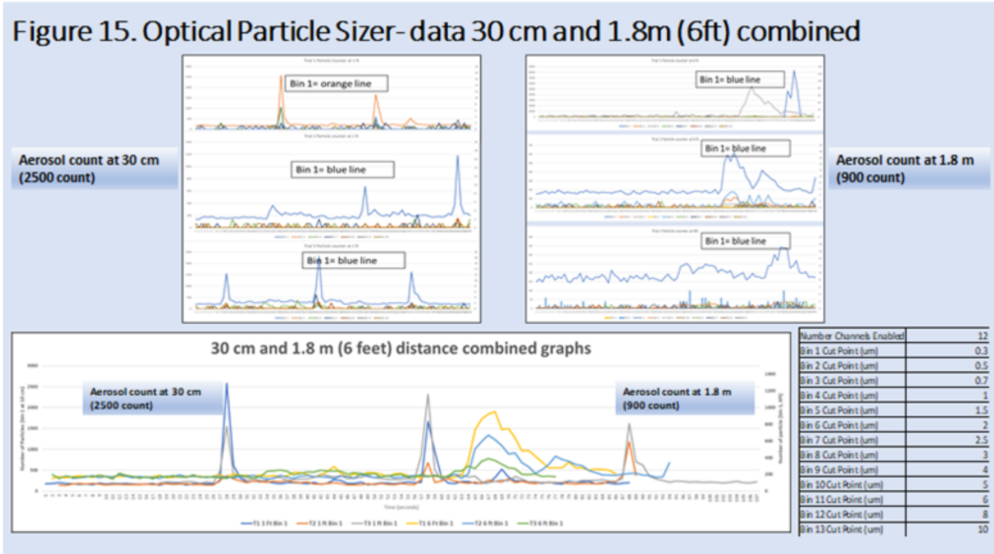


Figure 15. Shows the optical particle sizer data from 6ft and 30 cm away from the BLAM.

The one-way ANOVA test between aerosol count at the ambient condition (without cough) and number of aerosol count at 30 cm and 1.8 m away was statistically significant. Specifically this occurred 30 cm away where, $F(2,87)=4.76$, $p<0.012$. This also occurred 1.8 m away where, $F(2,87)=4.18$, $p<0.018$, suggesting that the null hypothesis was rejected and that the data presented a statistical significance between the number of ambient particles and the number of particles, both 30 cm and 1.8 m (6ft) away after a cough, as shown in Figure 16.

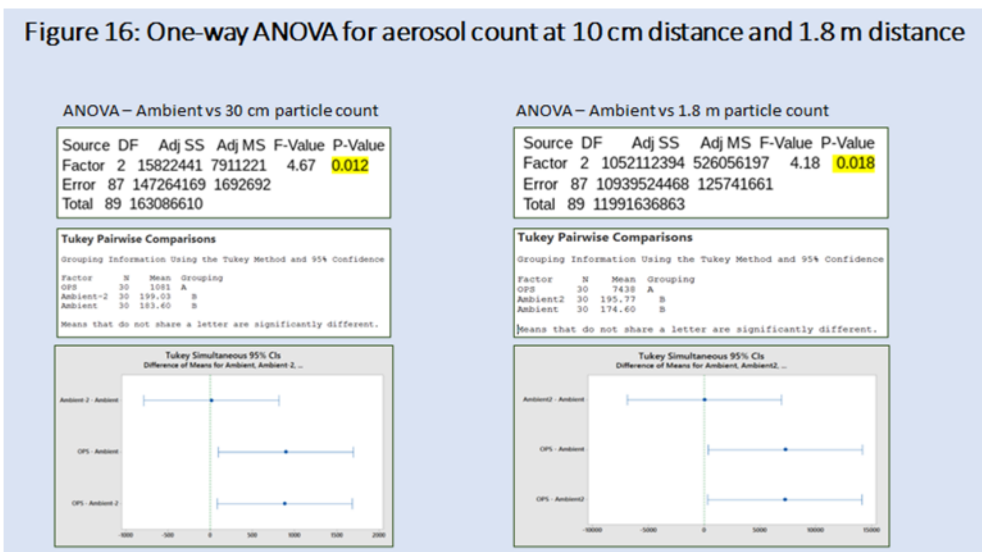


Figure 16 shows the one-way ANOVA completed to show that the particles can travel further than 6 ft.

**Part 4: Particle Image Velocimetry:**

Lastly, as shown in Figure 17, images through the particle image velocimetry were taken to analyze the velocity vectors of the particle and image frames.

In addition, these images were sequenced, and a region of interest was selected on MATLAB's PIVlab processor. The data was then analyzed with an interrogation area of pass 1 at 30 px and pass 2 at 10 px and set into a velocity magnitude profile as shown in the bottom of Figure 17. With the help of PIVlab, it was found that the maximum velocity of a cough can range between 6 - 28 m/s when cough flow velocity is approximated as a steady jet.

## Discussion and Recommendations

**Part 1:**

It was stated that the purpose of Part 1 of this experiment was, to accurately measure a cough's pressure characteristics. In this experiment, the sensors were able to detect the smallest changes in exhalation force and humidity of breath conditions via cough or sneeze, therefore, accurately quantify intensity, and frequency with any external disruptions of the patient's pre-existing conditions of pulmonary biomarkers such as dry cough, weezing, and bouts. The actual cough signal, when matched to the signal generated from controlled pressure release of a compressed air valve, can provide a reliable method to experimentally simulate cough using CSM-eStep and BLAM orifice. *This experiment was successful in simulating the cough and the engineering goal was met*. From part 1 cough data when matched with sensor signal of the air pressure test, it was noticeable that for

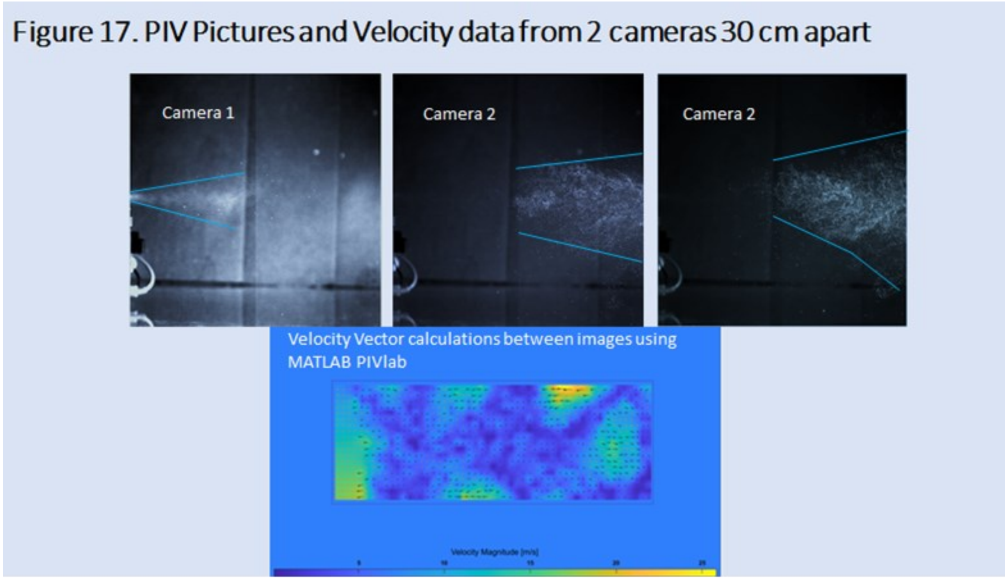


Figure 17. PIV Pictures and Velocity data from 2 cameras 30 cm apart

Figure 17 shows the PIV pictures with particle trajectory and MATLAB PIVlab velocity vector calculations.

SK (teenager) the closest match was at 30 PSI. Similarly the cough from AK (adult) participant the closest pressure match was at 40 PSI. This showed that AK (adult participant) had a higher intensity cough, while SK (teenage participant) had a lower intensity cough. Also from the graph it is clear that no two coughs are similar in intensity for either an adult or a teenager thereby confirming the variations in cough pattern depending on the exhalation or ailment conditions. It can also be concluded that adult coughs generate higher amounts of aerosol humidity thus providing clear evidence that when the virus host is an adult, the probability of airborne disease transmission is highly likely. Since the lung volume, capacity, and exhalation pressure vary for person to person, it was broadly concluded that between 30-50 PSI of compressed air release would be a simulated measurement for a human cough.

Many researchers have developed quite complicated systems to fully evaluate the forced exhaled breath conditions, such as, a cough or a sneeze. Experiments published in the *Physics of Fluids* journal used a complicated double pass Schlieren setup for imaging human coughs and the subject had to continuously exhale for a period of time (Simha and Rao, 2020). Such measurements are only limited to patients that have the ability to be able to predict the onset of their medical condition and have to be able to continuously blow air to perform such expensive tests. These limitations can easily be overcome using CNT fast response flex and humidity sensors where the subject can be in any pulmonary condition and be of various age groups. This quantification of cough intensity is very important in understanding the flow pattern of the airborne pathogen traveling in air or indoor environment. One limitation of this research is that there were only two human participants in the study. For the future, a bigger sample size could further enhance the data validity.

**Part 2.**

For Part 2 of this experiment, it was stated that, "when CNT flex sensors are placed at gradually increasing distance from a CSMe-STEP (cough simulator) and BLAM atomizer, then the sensor's signal pattern will be able to accurately measure a cough's pressure and aerosol decay over increasing distance." This experimental trial demonstrated the air flow transitioning from laminar to turbulent flow by measuring the signal dissipation, as shown in Figure 11 and 12, therefore, meeting this engineering goal. When the sensors were moved away from the BLAM orifice in increasing steps of every 10 cm, there was a non-linear increase in the average time it took for the pressurized air puff to bend the two sensors 30 cm apart. This shows that as the distance increases, the kinetic energy of flowing air tends to decrease and diffuse rapidly, resulting in a decreasing deflection of the flex sensor. *The time gap from the first sensor to the second sensor was also increasing drawing to a conclusion that supports the engineering goal*.

Through experiments published in *Physics of Fluids,* researchers have been able to demonstrate this phenomenon only by sophisticated PIV systems and then translating this to an image processing software to calculate the time taken for the sneeze or cough ejecta travel (Dbouk et al., 2020). Agrawal et al. have shown in their research from mathematical calculations that the cough cloud travel lasts between 5s and 8s with a maximum time up to 14 s and the travel distance of 1.5 m to 3 m is easily achieved. Wei et al, had found that the airflow expulsion period of cough is 0.5 s, while Sharfman et al., found in their research that the airflow expulsion lasted 0.3 s (Liu & Wei, 2016). *The conclusion of this research is that the cough of an adult was found to be in the range of 0.2 - 0.4 s.* This can be explained by the time that occurs after initial flow velocity. When a participant coughs, a high source of pulmonary pressure assists in carrying the large drops through the cough cloud. However, after the initial cough cloud disperses, the pressure or flow velocity begins to rapidly decrease and diffuse through all directions, causing the flex sensor to have a lower bend resistance as the distance is increased. In addition, since the pressure is dispersed and initial velocity of the pressurized air is drastically reduced from the onset of the cough cloud, it takes longer for the air to reach distances that are gradually increasing, therefore, increasing the travel time. This was shown by calculations using the velocity escaping compressed air formula. The initial velocity of the pressure released from the orifice was calculated to be greater than 300 m/s, however, after 0.2 - 0.4 seconds, the pressure drastically dropped to 5 m/s to less than 0.9 m/s.

**Part 3:**

For Part 3 of this experiment, an analysis was completed to understand the dispersion of the aerosols. One-way ANOVA tests completed on the recorded data between the ambient conditions and simulated cough conditions shows that there was a p-value less than 0.015 for both 10 cm and 1.8 m distance. Since the p-value was less than 0.01, the null hypothesis can be rejected stating that there was a significant difference in the amount of aerosol particles after a participant coughs from a distance of 30 cm and 1.8 m, in relative to the ambient number of particles without the cough spray. Current guidelines, as stated by the CDC, to follow proper social distancing guidelines, people from different households should remain at least 6 feet (1.8 meters) apart, especially if a mask is not worn. As shown in Part 3 of this experiment, there were a significant number of particles that can travel beyond 6 ft. Further, this shows that a distance larger than 6ft (1.8m) should be maintained during cough or high stress exhalation to help halt the spread of the Sars-CoV-2 virus, as enhancement to current CDC guidelines. There has been a lot of research completed on understanding how far particles can travel, however, the research only consists of using various mathematical models to predict the projection of the large droplets and aerosols based on predicted aerosol sizes. For example, a study published in the *Journal of Fluid Mechanics* focused on creating a mathematical formula to predict the curvilinear projection of aerosols after the cough cloud has dispersed for various particle sizes. The researchers were able to predict that the aerosols can travel up to 6.7 m. While, another study published in the *Journal of Physics of Fluids,* used the Gaussian mathematical function to predict how far aerosols can travel after dispersion from a cough cloud when a mask is not worn. The researchers, Agarwal et al., predicted that in ambient conditions, the aerosols can travel between 1.5-3m (Agrawal et al., 2020). Lastly, another paper published in the *Journal of Physics of Fluids,* by Dbouk et al., used a series of conservation equations and computed droplet velocity using Newton's second law of motion, to predict that aerosols in environmental conditions with no wind influence do not travel farther than 1 m (Dbouk et al., 2020). Although the researchers were able to predict the velocity and trajectory of particles and aerosols using mathematical modeling, their results were accompanied with many limitations due to lack of actual experimentation with ultra-fast sensors. In addition, most researchers arrived at different aerosol travel distance conclusions. This research, however, was able *to successfully bridge that gap and complete experimental trials to understand the aerosol trajectory*. It was found that the particles ranging in sizes between 0.3-0.5μm can travel further than 6 feet. A significant source of error while collecting particle sizer data was that the mount that held the carbon nanotube sensors potentially could have stopped different aerosol particles from reaching one of the particle sizers.

**Part 4: PIV**

It was stated that Part 4 of this experiment was to use the PIV to take highspeed pictures of the simulated cough from the orifice and analyze the data in MATLAB's PIVlab to calculate the velocity vectors from the PIV images. Cough, as stated earlier, is a multiphase compressed air jet carrying large quantities of pathogen bearing large droplets, droplet nuclei, and aerosols. In this experiment the results of the PIV showed droplets exiting the orifice simulating the calibrated human cough. This is also confirmed by the calculated velocity vectors through PIVlab and flex sensor time delay velocity calculations. These images clearly show the linear jet cone projection in time elapsed references and the spread of qualitative characteristics of particle sizes, locations, and particle distribution. As seen in the images, as time elapses (0.1 to 3 s), this linear jet gradually translates to a wider cone shaped cloud. Based on the comparison between the PIV and the optical particle sizer aerosol distribution, it can be concluded that many tiny aerosol particles travel further than 1.8 m (6 ft). The indoor conditions with HVAC air speed can further influence the aerosol trajectories carrying airborne diseases rendering the 1.8 m social distancing rule insufficient. The shortcoming of this experiment is that the droplets or aerosol are spherical in shape and in reality, the viscosity of saliva creates ligaments and odd shaped suspended aerosol. Lastly, as depicted by Figure 17, not only do the aerosol particles travel in a linear pattern, however, many large droplets fall due to gravitational influence and particles can also travel, not only forward, but also backwards. In the future, it would be beneficial to further analyze the different directional flows of the aerosol particles using PIVlab.

*In conclusion, based on the 4 part trials, this research was able to successfully simulate human cough, measure the cough intensity and quantify its flow characteristics and velocity and pressure decay.* The results clearly show that there is a large quantity of droplet and aerosol ejected from cough that travel significantly further than the 1.8 m social distancing guideline as recommended by CDC. It also confirms that whether it be indoor or outdoor conditions, these pathogen laden aerosols settle on various surfaces, therefore, *requiring a thorough sanitization process* which is not enforced under CDC guidelines. For the future, it would be key to understand how aerosol particles travel through different indoor environmental conditions, such as varying humidities, temperatures, and HVAC flow path. In addition, as this study focused on understanding the velocity characteristics of a cough, it would be beneficial to understand different modes of virus transmission, such as sneezing and talking. Not all parameters of this experiment that stimulated a cough are representative of an actual human cough with respect to the released amount of aerosol volume. Lastly, this project was only representative of two subjects in healthy conditions and their cough variance. It would also be beneficial to understand how cough pressure varies between different physiological conditions and a large number of participants.

## References


Agrawal, A., & Bhardwaj, R. (2020). Reducing chances of COVID-19 infection by a cough cloud in a closed space. *Physics of Fluids, 32*(10), 10.1063/5.0029186. doi:https://doi.org/10.1063/5.0029186

Bourouiba, L., Dehandschoewercker, E., & Bush, J. (2013, December 01). Violent expiratory events: On coughing and sneezing. Retrieved January 30, 2021, from https://dspace.mit.edu/handle/1721.1/101386

Cough. (n.d.). Retrieved January 30, 2021, from https://www.nhlbi.nih.gov/health-topics/cough

COVID-19 Map. (n.d.). Retrieved November 22, 2020, from https://coronavirus.jhu.edu/ map.html

Dbouk, T., & Drikakis, D. (2005). Https://www.e-unwto.org/doi/book/10.18111/9789284408047. *Physics of Fluids, 32*(5), 10.1063/5.0011960. doi:10.18111/9789284408047

Electrical4U. (2020, October 28). Sensor: Types of Sensor. Retrieved November 14, 2020, from

https://www.electrical4u.com/sensor-types-of-sensor/

Engineers Edge, L. (2017, September 18). Velocity Escaping Compressed Air Equation and Calculator. Retrieved January 30, 2021, from https://www.engineersedge.com/fluid_flow/velocity_escaping_14031.htm

Jon Greenberg, P. (2020, October 08). What We Know About the Airborne Spread of the Coronavirus. Retrieved November 22, 2020, from https://khn.org/news/fact-check-airborne-transmission-coronavirus-science-behind-aerosol-spread/

Liu, L., Wei, J., Li, Y., & Ooi, A. (2016, March 23). Evaporation and dispersion of respiratory droplets from coughing. Retrieved January 30, 2021, from https://onlinelibrary.wiley.com/doi/abs/10.1111/ina.1229

Lowen, A. C., Mubareka, S., Steel, J., & Palese, P. (2007). Influenza virus transmission is dependent on relative humidity and temperature. *PLoS pathogens*, *3*(10), 1470–1476. https://doi.org/10.1371/journal.ppat.0030151

Lu, L., & Sick, V. (2013). High-speed particle image velocimetry near surfaces. *Journal of visualized experiments : JoVE*, (76), 50559. https://doi.org/10.3791/50559

Morawska, L., & Cao, J. (2020). Airborne transmission of SARS-CoV-2: The world should face reality. *Environment international*, *139*, 105730. https://doi.org/10.1016/j.envint.2020.105730

Nishimura, H., Sakata, S., & Kaga, A. (2013). A new methodology for studying dynamics of aerosol particles in sneeze and cough using a digital high-vision, high-speed video system and vector analyses. *PloS one*, *8*(11), e80244. https://doi.org/10.1371/journal.pone.0080244

Optical Particle Sizer 3330. (n.d.). Retrieved January 30, 2021, from https://tsi.com/products/particle-sizers/particle-size-spectrometers/optical-particle-sizer-3330/

Osborn, C. (2020, April 23). Types of Coughs. Retrieved January 30, 2021, from https://www.healthline.com/health/types-of-coughs

Ossola, A. (2015, August 24). Carbon Nanotube Implants Could Help Diagnose Medical Conditions. Retrieved from https://www.popsci.com/g00/special-carbon-nanotubes-could-help-

Personal and Social Activities. (n.d.). Retrieved November 14, 2020, from https://www.cdc.gov/coronavirus/2019-ncov/daily-life-coping/personal-social-activities.hTl

Stinchcombe, C. (n.d.). How Far Does a Cough or a Sneeze Travel? Asking for a Friend. Retrieved January 30, 2021, from https://www.self.com/story/germs-sneezing-coughing

Tang, R., Shi, Y., Hou, Z., & Wei, L. (2017). Carbon Nanotube-Based Chemiresistive Sensors. Sensors,17(4), 882. doi:10.3390/s17040882

Qian, H., & Zheng, X. (2018). Ventilation control for airborne transmission of human exhaled bio-aerosols in buildings. *Journal of thoracic disease*, *10*(Suppl 19), S2295–S2304. https://doi.org/10.21037/jtd.2018.01.24

Rosa, G. L., Fratini, M., Libera, S. D., Iaconelli, M., & Muscillo, M. (2013n.d.). Emerging and potentially emerging viruses in water environments. Retrieved from https://scielosp.org/pdf/aiss/2013.v49n2/124-132/en

Staff, S. (2014, March 31). Carbon nanotubes find real world applications. Retrieved August 30, 2020, from https://phys.org/news/2014-03-carbon-nanotubes-real-world-applications.html

Yang, W., Elankumaran, S., & Marr, L. (2012). Relationship between humidity and influenza A viability in droplets and implications for influenza's seasonality. Retrieved November 14, 2020, from https://www.ncbi.nlm.nih.gov/pmc/articles/PMC3463543

Yuguo, W. (2017). Human Cough as a Two-Stage Jet and Its Role in Particle Transport. Retrieved January 30, 2021, from https://pubmed.ncbi.nlm.nih.gov/28046084/#:~:text=Human%20Cough%20as%20a%20Two-Stage%20Jet%20and%20Its,the%20transmission%20of%20respiratory%20diseases%20in%20indoor%20environments

## Appendix A:

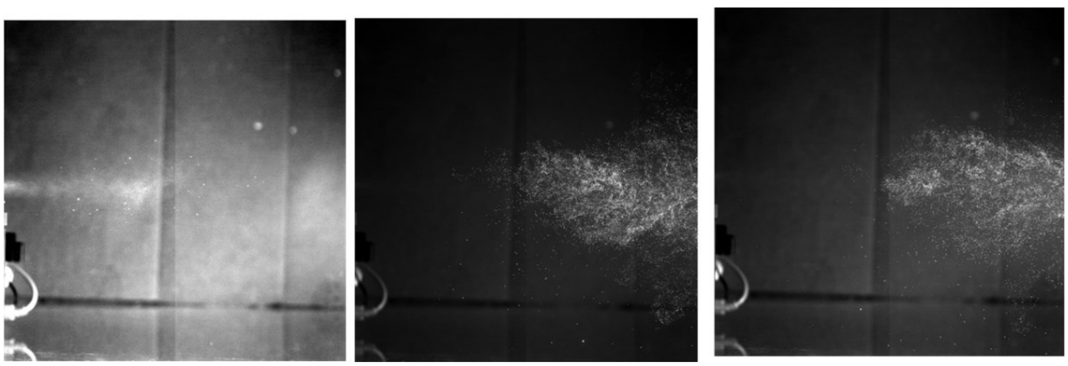

Appendix A depicts images of viral aerosol particles collected from the PIV.